537.525.6

PULSED NANOSECOND ELECTRIC DISCHARGES IN GASES

G. A. MESYATS, Yu. I. BYCHKOV, and V. V. KREMNEV

Institute of Atmospheric Optics, Siberian Division, USSR Academy of Sciences, Tomsk

Usp. Fiz. Nauk 107, 201–228 (June, 1972)

We analyze the physical phenomena occurring during the breakdown of gas gaps within times on the order of several nanoseconds or less. It is noted that the streamer mechanism has low probability if the times of formation of the discharge and the fall-off of the voltage across the gap are commensurate with the emission times of the excited molecules. The development of a Townsend discharge is made difficult by the strong influence of the space charge of the avalanche. The discharge mechanisms in single-electron and multi-electron initiation are described and the features of their development are outlined. Oscillographic and electron-optical measurement procedures are described and the main experimental results are reported. Theories explaining the main regularities are presented together with the mechanism for initiation and development of a discharge in ultrastrong electric fields. It is noted that x-radiation is produced in the discharge. Results are reported on a discharge at a voltage below the static breakdown value, initiated by fast electrons and by intense ultraviolet radiation.

CONTENT

1. INTRODUCTION

PULSED breakdown in the nanosecond and subnanosecond time region is of interest because the time of discharge development becomes commensurate with such elementary-process times as the time of growth of the avalanche to the critical dimension and the time of emission of the excited molecules. This circumstance leaves its imprint on the spatial structure of the discharge on the statistics of the delay, on the value of the delay time, etc.

At gas pressures (air, nitrogen, CO_2, etc.) on the order of several atmospheres and more such a discharge differs sometimes from an ordinary discharge in the absence of a discharge channel even though the discharge current reaches in some cases 10^5A. The rate of current growth in such a discharge is therefore not always determined by the processes occurring in the channel, and the channel stage does not play the same role as in an ordinary discharge. The formation of spark channels in the gap can occur already after the current has reached its maximum value, and several channels (sometimes on the order of several dozen) can be produced instead of one channel. Most investigations of pulsed nanosecond discharges therefore do not deal with the channel stage.

If the pulse duration is made shorter than the time necessary for channel formation, the channel stage can be avoided completely. In the present review we therefore neglect for the most part the channel stage. This type of discharge in a high-pressure gas is of great interest for numerous practical applications, such as the construction of powerful nanosecond pulsed devices, gas lasers with high gas pressure, generation of powerful electron beams, etc. Let us examine the position occupied by the nanosecond pulsed discharge among other discharges.

The development of a discharge in a gas usually begins with the appearance of initiating electrons at the cathode, followed by formation of avalanches of electrons and ions. The growth of the number of electrons and ions in the avalanche is exponential:

$$N = N_0 e^{\alpha x}, \quad (1)$$

where N_0 is the number of initial initiating electrons, α is the coefficient of impact ionization, and x is the path traversed by the head of the avalanche.

When the number of avalanche electrons reaches a certain critical value N_c, the field of the electron and ion space charges becomes comparable with the applied field, and the exponential growth of the number of charges slows down. The critical length of the avalanche is then determined by the formula

$$x_c = \ln N_c/\alpha$$

(it is assumed that $N_0 = 1$).

The character of the discharge in the gas depends essentially on whether the avalanche can acquire N_c electrons over the length of the gap d, i.e., it depends[1,2] on the relation between x_c and d. If $x_c > d$, then a single primary cascade is insufficient to complete the discharge, and secondary and subsequent avalanche, which are produced from the secondary electrons, must take part. This type of discharge is customarily called a Townsend discharge. If $x_c < d$, then the dominant role in the development of the dis-

charge is played by the primary avalanche, which goes over into a streamer and then into a discharge channel, This is called a streamer discharge.

For a streamer discharge to exist it is necessary, in addition, that the avalanche radiate enough photons to ionize the gas molecules near the head of the avalanche. The photons emitted by the avalanche are due to de-excitation of the excited gas molecules[3], the lifetime τ_{exc} of which is usually 10^{-9}—10^{-8} sec[3]. Therefore if the time t_c needed for the avalanche to reach its critical dimension is shorter than τ_{exc}, the development of the streamer from the primary cascade will be difficult. The formation of the discharge is then governed by processes which will be considered later on. The value of t_c is determined from the relation

$$t_c = \ln N_c/\alpha v_-,$$

where v_- is the electron drift velocity in the avalanche. Consequently, the conditions for the existence of a streamer discharge can be written in the form

$$\ln N_c/\alpha < d, \quad \ln N_c/\alpha v_- > \tau_{exc}.$$

According to the data of[3], the value of τ_{exc} for nitrogen at atmospheric pressure is ~3 nsec and $\ln N_c \approx 20$. Consequently one can expect the discharge for properties to deviate from those of a streamer discharge already at $\alpha v_- \geq 10^{10}$ sec^{-1}, i.e., at $E > 6 \times 10^4$ V/cm.

The development of a pulsed discharge in a gas is strongly influenced by the current i_0 of the initiating electrons, and also by the degree of homogeneity of its distribution over the cathode surface. When estimating the influence of i_0 on the discharge process, it is convenient to compare the average time between the appearance of two electrons from the cathode e/i_0 (e is the charge of the electron) with the time t_c of avalanche development to the critical dimension. If $t_c < e/i_0$, then it can be assumed that the discharge is initiated by single electrons, in which case

$$i_0 < e\alpha v_-/\ln N_c.$$

When the current i_0 is increased, the secondary processes play a lesser role in the growth of the discharge current. If the time necessary for the avalanche to develop the critical dimension is $t_c \gg e/i_0$, i.e.,

$$i_0 \gg e\alpha v_-/\ln N_c,$$

and the current i_0 is uniformly distributed over the cathode, then the simultaneous development of a large number of electron avalanches gives rise to large currents even before the secondary processes begin to act.

When the electric field is increased to $E > 10^5$V/cm, the development of the discharge begins to be strongly affected by microscopic bumps on the surface of the cathode, at which the fields can increase by a factor of 100 and more. As will be shown in Sec. 3a, this leads to emission of electrons from local spots on the cathode, and when a definite field value is exceeded it leads to explosion of such bumps. Whereas the electric field intensity in the gas gap can reach 10^6V/cm, it can amount to 10^8V/cm at the microscopic bump. The time necessary to explode a sharp point of tungsten is on the order of 10^{-9} sec. The explosion produces a cathode-metal plasma, which helps increase the electron current from the cathode.

The principal information concerning the processes occurring in a nanosecond discharge is usually obtained from oscillograms of the spark current and voltage. In analogy with an ordinary pulsed discharge in a gas, we shall use such terms as the discharge delay time and the discharge formation time, taking the start of the discharge to mean the start of the rapid growth of the current in the gap and of the decreased gap voltage. It must be remembered, however, that the formation of the discharge usually continues even after the current begins to grow. From the methodological point of view, it is more convenient in the experiments to measure separately the time during which the current reaches several amperes and the time during which the current increases from several amperes to the nominal value. These quantities are also easier to determine analytically.

The purpose of the present review is to summarize the research on discharges in gases at electric field values higher than those in which the streamer discharge mechanism operates, i.e., at $\alpha v_- > \ln N_c/\tau_{exc}$. The characteristic development times of such a discharge amount to nanoseconds and fractions of a nanosecond. Such a discharge can be produced by applying to the gas a rectangular voltage pulse with amplitude greatly exceeding the static breakdown voltage and with a rise time shorter than the characteristic discharge development time. We shall not deal with nanosecond discharges in static breakdown, in which the discharge time is decreased by increasing the gas pressure. These questions are discussed in detail in the reviews[4,5].

Since the principal role in the process of pulsed nanosecond discharge is played by electron avalanches, we shall examine, before we proceed to describing the discharge process under various conditions, the behavior of a single electron avalanche in a gas in the case of strong electric fields and large values of E/p.

2. DEVELOPMENT OF ELECTRON AVALANCHES IN A GAS IN STRONG ELECTRIC FIELDS

a) **Principal physical parameters determining the development of electron avalanches.** Discharge in a gas begins with the development of an electron avalanche. To understand the development of a discharge of one type or another it is therefore necessary to understand, at least in general outline, the features of the development of electron avalanches under the conditions of discharges of this type. The development of electron avalanches under the conditions of the existence of a Townsend or a streamer discharge were analyzed in detail by Raether and co-workers[3].

The discharge considered in the present paper exists at gas pressures on the order of atmospheric and higher, and at fields intensities up to 10^5 V/cm and higher. Under such conditions, the characteristic times of the development of electron avalanches do not exceed 10^9 sec, thus making their experimental investigation very difficult. The situation is made easier by

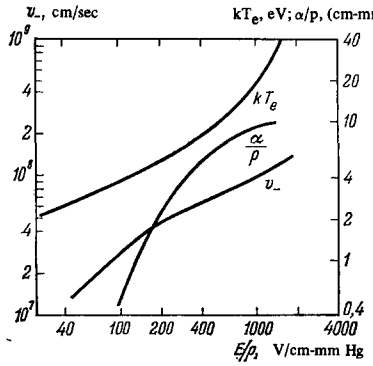

FIG. 1. Experimental plots of α/p, v_- and kT_e against E/p.

the fact that the main parameters determining the development of the electron avalanche, such as the ratio of the coefficient of impact ionization to the pressure α/p, the thermal energy of the electrons kT_e, and the electron drift velocity v_- depend only on the ratio E/p, and not on E or p separately[6]. Therefore the experimental results obtained earlier for electron avalanches at low field intensities E and low pressures p can be used for avalanches that develop at high field intensities E and high gas pressures.

Figure 1 shows plots of α/p, v_- and kT_e as functions E/p for nitrogen and air. The experimental plot of α/p against E/p, for air in the range $40 < E/p < 140$ V/cm-mm Hg is satisfactorily approximated by the formula

$$\alpha/p = A\,[(E/p) - B_0]^2, \tag{2}$$

where $A = 1.17 \times 10^{-4}$ cm-mm Hg-V^2 and $B_0 = 32.2$ V/cm-mm Hg.[1] The empirical relation for the drift velocity of electrons in nitrogen at $130 < E/p < 300$ V/cm-mm Hg is given by[7]

$$v_- = C\,(E/p)^{1/2}, \tag{3}$$

where $C = 3.3 \times 10^6$ $cm^{3/2}$ $(mm\ Hg)^{1/2}/sec\text{-}V^{1/2}$, and for $130 > E/p > 10$ V/cm-mm Hg we have

$$v_- = C_0\,(E/p), \tag{3'}$$

where $C_0 = 3.3 \times 10^5$ cm^2-mm Hg/sec-V. For air, the dependence of v_- on E/p is close to (3) and (3')[1].

Diffusion causes "smearing" of the electron cloud in the gas and its expansion. The radius of the electron cloud is usually defined as the distance from the center of the cloud to the point at which the electron density is decreased by a factor 2.72:

$$r_D = (4Dt)^{1/2}, \tag{4}$$

where D is the electron diffusion coefficient.

The electron diffusion coefficient is given by the well known formula

$$D/\mu = kT_e/e,$$

where μ is the electron mobility, kT_e is the thermal energy of the electrons, and e is the electron charge. The dependence of kT_e/e on E/p for nitrogen in the range $20 < E/p < 100$ V/cm-mm Hg is approximated by the formula[8]

$$D/\mu = kT_e/e \approx C_2\,(E/p)^{2/3}, \tag{5}$$

where $C_2 \approx 0.2$ $(V^{1/2}$ cm-mm $Hg)^{2/3}$.

The photons emitted by the excited molecules from the avalanches in the gas greatly influence the mechanism of the gas discharge. The radiation from the avalanches leads to photoionization of the gas, to a photoeffect on the cathode, and thus to the production of secondary electrons. Direct measurements of the emission spectra of avalanches with the aid of a vacuum spectrograph[9] have shown that intense lines in oxygen have wavelengths λ = 988, 888, 880, and 835 Å. Lines with wavelength shorter than 1000 Å were observed in nitrogen.

The emission of the ionizing radiation is characterized by the following parameters: ω [cm^{-1}]—the number of gas-ionizing quanta produced by an electron on a path of 1 cm; δ [cm^{-1}]—total number of quanta produced by an electron on a path of 1 cm; ω/α—number of ionizing quanta per electron in the avalanche.

The parameters of ionizing radiation were measured in[10-12]. The radiation source used in[11,12] was in incomplete discharge in a homogeneous field. This has made it possible to trace the dependence of different radiation parameters on E/p in the gas discharge. It was observed that in pure oxygen ω/α increases with increasing E/p. This was attributed to the decrease in the radiation wavelength with increasing E/p.

The ionization potential of oxygen in air is lower by ~3.5 eV than the ionization potential of nitrogen, and therefore the photons emitted by the nitrogen ionize the oxygen. With increasing E/p, the coefficient α of impact ionization of air increases more rapidly than the coefficient ω, and therefore ω/α decreases with increasing E/p[11].

It follows from[13] that in air each electron of the avalanche produces on the average 0.4 photon in the range pd = 20—120 cm-mm Hg (d = 1 cm), at wavelengths $\lambda > 2000$ Å, and at E/p = 50—80 V/cm-mm Hg. The excited gas molecules emit photons after an average time τ_{exc}. The value of τ_{exc} decreases with increasing gas pressure owing to the collisions that quench the excitations. The data of[14] give for nitrogen

$$\tau_{exc} = \tau_{exc}[1 + (p/p_0)]^{-1},$$

where $\tau_0 = 36 \pm 3$ nsec and $p_0 = 60 \pm 6$ mm Hg.

Let us estimate the influence of the electric field intensity in the gap on the number of photons leaving the avalanche by the instant of time when the number of electrons in the latter is N_c. We assume that when the number of electrons is $N < N_c$ the avalanche develops exponentially, and the expansion of the head of the avalanche is due to free diffusion. If the critical electron number N_c is determined from the condition that the external field be equal to the ion space-charge field, then[15] $N_c \sim T_e\alpha^{-1}$. Since α increases with increasing E more rapidly than the electron temperature T_e, it follows that N_c decreases with increasing electric field intensity. This effect, together with the decrease of the photon yield from the avalanche as the result of the short time of avalanche development, leads to a sharp decrease of the photon yield from the avalanche at E. Indeed, the number of excited molecules in the avalanche is $N_{exc} \sim N_c \sim T_e\alpha^{-1}$. But if $t_c \ll \tau_{exc}$, then the photon yield is

$$N_{ph} = N_{exc}\,t_c/\tau_{exc} \sim \alpha^{-2}v_-^{-1}T_e.$$

Substituting there the values of α, v_-, and T_e from (2), (3), and (5) we find that the number of photons N_{ph} decreases strongly with increasing electric field intensity E.

b) **Development of electron avalanches at large gains.** The fundamental relations (1) and (2)–(4), which determine the development of the electron avalanche, are valid only when the number of electrons in the avalanche is small and the avalanche space-charge field is much weaker than the external field. An analysis of the development of an electron avalanche at a large value of the gain, with allowance for the field of the electron cloud itself and for diffusion, is given in[16,17]. The development of an avalanche in helium was calculated numerically for E/p = 10 V/cm-mm Hg and p = 760 mm Hg, with $D = 4.7 \times 10^3$ cm^2/sec and $v_- = 5 \times 10^6$ cm/sec[18]. It was shown that at $N \geq 10^8$ the electrostatic repulsion of the electrons becomes significant.

A detailed investigation of the development of cascades was carried out by electron-optical and oscillographic methods in[19,20] for avalanches in ether and in nitrogen. It was found that at $N > 10^6$ the growth of the number of electrons is slower than the exponential growth (1). This phenomenon was explained in[17], where the influence of the ion field on the development of the electron avalanche was estimated by approximately solving the one-dimensional Poisson equation and the Townsend equation with allowance for the electron drift and spatial diffusion. The diffusion coefficient and the drift velocity of the electrons were assumed constant, and the transverse component of the ion and electron space-charge field was disregarded. The impact-ionization coefficient was assumed to depend linearly on the field. It was shown that the effective coefficient of impact ionization α_{eff} decreases with increasing number of electrons in the avalanche[17]:

$$\alpha_{eff}/\alpha_0 = 1 - \lambda N, \tag{6}$$

$$\lambda = (d\alpha/dE_0)\,(e/4\pi\varepsilon_0)\,F\,(\alpha_{eff} r_d)/\alpha_0 r_d^2, \tag{7}$$

where $F(\alpha_{eff} r_d) \approx 0.16$[19] for $0.4 \leq \alpha r_d \leq 2.5$; $\epsilon_0 = 1/4\pi \times 9 \times 10^{11}$ F/cm, and α_0 is the coefficient of impact ionization at $E = E_0$. The dependence of $\alpha_{eff}(N)$ calculated in accordance with (6) for nitrogen and ether was in satisfactory agreement with the experimental data[19,20] at $N \approx 10^6$–10^7, and the radius of the avalanche, calculated in accordance with (6) and (7) agreed with the experimental values.

At $N > 10^8$, the dependence of α_{eff}/α_0 on N becomes stronger[19,20] than in (6). In addition, the experimental dependence of α_{eff}/α_0 on N has at $N \approx 10^8$ a minimum that reaches 0.5. At these values of α_{eff}, the $\alpha(E)$ dependence deviates from the linear approximation used in the derivation of (6).

It should also be noted that the experimental data on avalanches with 10^6 electrons and more were obtained only for $10 < E/p < 200$ V/cm-mm Hg with $20 < p < 500$ mm Hg, when the avalanche development time was $t \geq 10^{-8}$ sec. At a pressure p on the order of one atmosphere and in fields $E \geq 10^5$ V/cm, the avalanche develops within a time $\sim 10^{-9}$ sec and less. There has been no experimental investigation of avalanches in this range of times.

To explain the character of the avalanche development in nitrogen at atmospheric pressure and at high electric field intensity, the fundamental equations for the development of the electron cloud were solved numerically. The calculations took into account the influence of the transverse component of the electric field of the avalanche, the dependence of the drift velocity and of the impact ionization coefficient α on the local field E at each point of space, and the ion velocity was assumed equal to zero; the electron transport equation, the continuity equation, and the Poisson equation are given by[16]

$$\mathbf{J} = -De\nabla n_- + \mathbf{v}_- e n_-, \tag{8}$$

$$e\frac{\partial n_-}{\partial t} + \nabla \mathbf{J} = \alpha \mathbf{J}, \tag{9}$$

$$\nabla \mathbf{E} = e(n_+ - n_-)/\varepsilon, \tag{10}$$

where $\mathbf{J}$, α, and $\mathbf{v}_-$ are the vector values of the current density, the impact-ionization coefficient, and the electron drift velocity, ∇ is the Hamilton operator, and ϵ is the dielectric constant of the medium. The values of α, v_-, and D were determined from formulas (2), (3), and (5).

The electric field $\mathbf{E}$ is the vector sum of the applied field and of the field produced by the space charges of the ions and the electrons. The diffusion and mobility coefficients were assumed constant in the calculations, and the directions of the vectors α and $\mathbf{J}$ were assumed to be the same. It was assumed in the calculation that $v_- \gg \alpha D$, which holds true for air, nitrogen, and ether at $E/p < 400$ V/cm-mm Hg. The initial values of the densities n_- and n_+ were those obtained by simultaneously solving Eqs. (8)–(10) without taking the space charge into account.

To verify the correctness of the chosen avalanche model, the system (8)–(10) was solved for ether vapor under the condition E/p = 200 V/cm-mm Hg and p = 21 mm Hg, for which there are experimental data on the avalanche parameters at large gains[19]. The results of the numerical calculation for the normalized electron density in ether in the longitudinal and transverse cross sections of the electron cloud are shown in Fig. 2 for ether (a and b) and for nitrogen (c and d). The following normalized parameters were used in the figure: the electron density

$$n = 8\,(\pi D/\alpha_0 v^{(0)})^{3/2} \exp\,(-\alpha_0 v^{(0)} t_0)\, n_-$$

and the coordinates

$$x,\ y = 0.5\,(\alpha_0 v^{(0)}/D)^{1/2}\,(z,\ r).$$

The numbers on the curves indicate the normalized

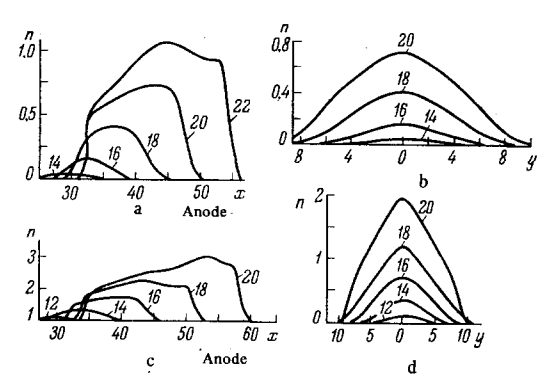

FIG. 2. Normalized electron density in the head of an avalanche.

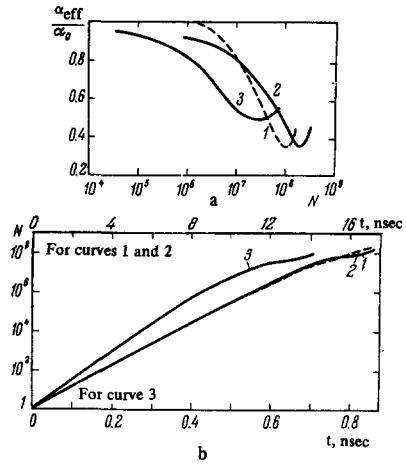

FIG. 3. a) Effective impact-ionization coefficient vs. the number of electrons in the avalanche; b) increase of number of electrons in the avalanche with time.

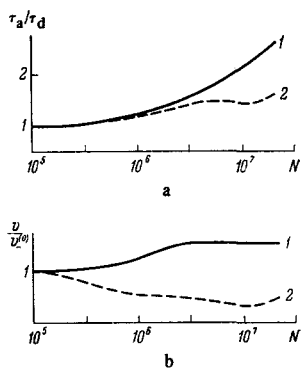

FIG. 4. a) Radius of avalanche in the longitudinal (1) and transverse (2) cross sections; b) electron velocity on the front (1) and in the "tail" (2) of the electron cloud.

time $\tau = \alpha v^{(0)}t$, where t is the time from the start of the initial electron. When comparing the experimental and calculated values of $\alpha_{eff}(N)$ and N(t), it was assumed that $D/\mu = kT_e/e = 3.26$ V in (10). α_{eff} was determined from the relation

$$N = \exp(\int \alpha_{eff}\, v\, dt),$$

where V was defined as the velocity of a point on the z axis, equidistant from the levels at which the electron density is smaller by a factor $e \approx 2.72$ than the maximum value. It turned out in this case that $v \approx v^{(0)}$.

Figure 3a shows the calculated (1) and experimental (2) plots of $\alpha_{eff}(N)/\alpha_0$, while Fig. 3b shows the calculated (1) and experimental (2) plots of N(t) for ether. In agreement with experiment, the $\alpha_{eff}(N)/\alpha_0$ plot has a minimum at $N \approx 10^8$, which verifies convincingly the correctness of the assumed avalanche model.

The satisfactory agreement between the calculations and experiments for ether[19] served as a justification for performing with the aid of Eqs. (8)—(10) an analogous calculation for air at p = 760 mm Hg, in order to explain the features of the development of a single avalanche in a strong electric field at $E = 10^5$ V/cm when the expected time of development of the avalanche to the critical dimension was less than 10^{-9} sec. The calculation was performed in accordance with the same program as for ether. A value $D/\mu \approx 4.4$ was assumed as in the case of nitrogen. Figure 3 (the two curves 3) shows the result of the calculation α_{eff} and N for air, from which it follows that a deviation from the exponential growth of the avalanche becomes observable at $N = 10^6$ already 0.4 nsec after the start of the avalanche development.

It is seen from the plots of the normalized electron density in the longitudinal and transverse cross sections of the electron cloud, shown in Figs. 2c and 2d, that the electron cloud becomes strongly deformed at large N. Figure 4a shows a plot of the ratio r_a/r_d for air in the case of the longitudinal (1) and transverse (2) cross sections of the electron cloud. The quantity r_a is defined as the distance between the outermost points of the cloud at which the density is 2.72 times smaller than the maximum value. The plots show that for air at $N > 3 \times 10^5$ the expansion of the avalanche exceeds the diffusion value, and at $N = 2 \times 10^7$ the radius of the electron cloud in the drift direction is approximately 2.5 times larger than the diffusion radius.

The maximum rate of expansion of the electron cloud in air (see Fig. 4a) transversely to its motion is approximately 10 times larger than the rate of expansion due to diffusion, and amounts to $\sim 0.5v_{\perp}^{(0)}$, and in the drift direction it amounts to $0.6v_{\perp}^{(0)}$. It follows from the plots in Figs. 2c and 2d that the electron cloud does not develop uniformly. For example, the rate of growth of the electron density in the "tail" of the cloud (see Fig. 2a) decreases, and the velocity of the drift to the anode in this region (Fig. 4b, dashed line) slows down. This is due to the growth of the plasma density between the electron and ion clouds and to the ensuing decrease of the electric field as the result of the mutual penetration of the electron and ion clouds. In the front part of the electron cloud (see Fig. 2c) to the contrary, there appears a region in which the density increases progressively with time, and which contains a section with a large radiant (the front of the cloud). The length of the front remains unchanged in the interval $15 < \tau < 20$. The solid curve in Fig. 4b is a plot of the drift velocity of a point on the front where the electron density is smaller by factor 2.72 than the maximum value, as a function of the number of electrons in the avalanche N. This velocity remains constant at $\sim 5 \times 10^7$ cm/sec or $1.5v_{\perp}^{(0)}$ for $N > 3 \times 10^6$, owing to the increase of the electric field on the front of the electron avalanche.

3. DISCHARGE INITIATED BY A SMALL NUMBER OF ELECTRONS IN GAS-FILLED GAPS

a) **Breakdown delay time and current of initiating electrons.** The very first experiments[1] on pulsed breakdown of gas-filled gaps have shown that a certain time t_{del} elapses between the application of the voltage pulse and the breakdown of the gap. In the general case, according to these experiments, the number n_t of breakdowns having a delay time t and longer depends on the delay time in the following manner:

$$n_t = n_0 e^{-(t+\tau)/\sigma_0},$$

where σ_0 is the average statistical delay time, n_0 is the total number of breakdowns, and τ is a certain minimal time below which the breakdown delay time

does not decrease under the given conditions. The breakdown delay time t_{del} consists of two components, statistical σ and the discharge-formation time τ, i.e.,

$$t_{del} = \sigma + \tau.$$

The value of σ is determined by the electron current from the cathode and has a statistical character to it. The connection between i_0 and σ_0 is given by[1]

$$i = e/\sigma_0 w_1 w_2,$$

where e is the electron charge, w_1 is the probability of occurrence of an electron in both regions of the gap where it can lead to breakdown, and w_2 is the probability that this electron will actually lead to a breakdown. The value of σ_0 is determined experimentally from the slope of the line $|\ln(n/n_0)| = (t - \tau)/\sigma_0$. For gaps with length on the order of several millimeters, with an overvoltage of 80% and more, we have $w = w_1 w_2 = 1$,[21] and consequently

$$i_0 = e/\sigma_0. \qquad (11)$$

Formula (11) is extensively used to determine the electron current. It follows from (11) that σ_0 is none other than the average time between the appearance of two initiating electrons. There exists a limit of the value of the current i_0, above which it cannot be determined from the slope of the line $|\ln(n/n_0)| = (t - \tau)/\sigma_0$. This occurs when $\sigma_0 < \tau$. Actually, owing to the usually present statistical saturations of the time τ, it is necessary to have $i_0 \ll e/\tau$ in the measurements.

Under conditions where there are no special auxiliary electron sources, the discharge is initiated by electrons produced by the cathode itself. The total intensity of the external radiation is usually negligibly small and is of the order of 10 electrons per second per cm^3 of air. We can indicate the following sources of initiating electrons from the cathode:

1. Electron emission due to dielectric films and inclusions on the surface of the cathode[22] (the Malter effect, or anomalous emission through dielectric films on the cathode, and the Paetow effect, or field emission enhanced by the charging of dielectric inclusions on the cathode. These effects are described in detail in[1,3]. The role of this emission is particularly large when easily-oxidizing cathodes are used.

2. Exoelectronic emission[23]. The density of the cathode exoelectron current from electrodes without special treatment usually does not exceed 100–1000 electrons/cm^2sec. Such a current can influence only breakdown by millisecond pulses.

3. Field emission. This type of emission is the main source of initiating electrons at $E_0 = 10^5$–10^6 V/cm.

To obtain from a tungsten cathode surface area of 1 cm^2 a field-emission current, 10^{-10} A, at which the statistical-delay time is of the order of 10^{-9} sec, it is necessary to have an approximate electric field intensity 2×10^7 V/cm. We are interested in a pulsed electric discharge in a gas at a field intensity 10^5–10^6 V/cm.

Numerous investigations of the pre-breakdown conductivity in a vacuum gap at $E = 10^5$–10^6 V/cm have revealed the presence of electron currents of 10^{-5}–10^{-3} A and a qualitative agreement between the dependence of this current on the average field intensity in the gap, on the one hand, and the Fowler and Nordheim formula for field emission[24], on the other. This is attributed to the presence of microscopic inhomogeneities on the surface of the electrode, at which the field intensity E greatly exceeds the average macroscopic field, defined in the case of flat electrodes as $E_0 = U_0/d$ (d is the gap length and U_0 is the potential difference across the gap). The ratio $E/E_0 = \mu$ is called the field gain.

For the case of a hemisphere on a surface or a small hill whose height is commensurate with its diameter, the value of μ does not exceed[25] 10. Frequently, however, these roughnesses take the shape of elongated points ("whiskers") and not of hills. The most illustrative in this respect are the experiments of[26-28], in which an electron microscope was used to study the electrode surface. It is possible to obtain a simple relation between the coefficient μ and the parameters of the projection, by assuming the projection to be a half-ellipsoid. If the parameters of the projection are taken to be the radius of curvature of its crest r and the height h, then[26]

$$\mu = (\beta h/r) + 1,$$

where β is a slowly and monotonically varying function of h/r: at h/r = 5–250 we have β = 1–0.4, i.e., it can be assumed approximately that $\mu \sim h/r$ at $h/r \gg 1$. Measurements of μ using smooth metallic surfaces at macroscopic fields on the order of 10^5 V/cm yielded $\mu \approx 20$–70[29,30] or $\mu = 10$–300[31,32].

There is direct proof that the surface of the cathode affects the delay time of the breakdown and the value of the breakdown field intensity when nanosecond pulses are applied to the gap. It was found in[33] that very smooth mechanical polishing of the cathode can increase the dielectric strength of an air gap of length less than 1 mm by several times and raise it to 1.4×10^6 V/cm at a delay time on the order of 10^{-9} sec.

At a pulse duration 40 nsec in air gaps of length ~0.2 mm, using single-crystal cathodes (molybdenum, tungsten, rhenium), the electric field intensity at which the breakdown takes place reached 3×10^6 V/cm, whereas for polycrystalline cathodes it did not exceed 1.3×10^6 V/cm[33,34]. In the same investigations[33,34], using a single-crystal cathode, the pulsed electric strength remained practically unchanged when the gas pressure was changed by several times. All these facts indicate that in pulsed breakdown of gases in strong electric fields the initiating electrons are produced by field emission.

b) Time of discharge formation. In pulsed breakdown of atmospheric air by rectangular pulses with a rise time of 0.3 nsec and $E \geq 10^5$ V/cm, the discharge-formation time τ in the case of a small current of initiating electrons from the cathode exceeded by one or two orders of magnitude the time required for the avalanche to develop to critical size[35].

A more detailed investigation of the time τ in atmospheric air following initiation by a small electron current was carried out in[36]. For each pulse amplitude, 100 oscillograms were taken and the func-

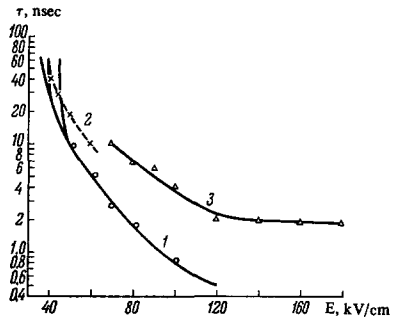

FIG. 5. Dependence of the discharge-formation time τ on the field intensity E. 1) Multielectron initiation: solid curve–from [37]; points–from [36]. 2) From [38]. 3) Single-electron initiation [36].

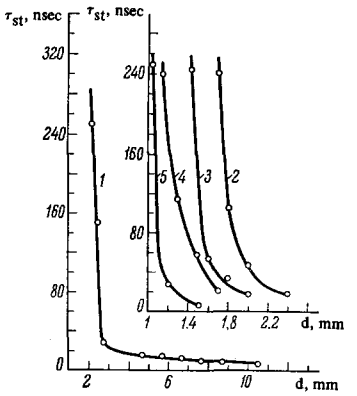

FIG. 6. Plot of τ_{st} against d (p = 760 mm Hg). E (kV/cm): 1–100; 2–125; 3–150; 4–175; 5–200.

tion $|\ln(n/n_0)| = f(t)$ was plotted (n is the number of breakdowns with delay time t and longer, and n_0 is the total number of breakdowns). The discharge-formation time τ was assumed to be the minimum time obtained in this distribution. The cathode-irradiation intensity was chosen such that the time σ_0 was commensurate with τ. The $\tau(E)$ dependence obtained in this manner is shown in Fig. 5 (curve 3). Curve 2 in the same figure was obtained under approximately analogous conditions[38].

It was noted in[35] that at E = const the time τ increases with decreasing gap length. This dependence was investigated more thoroughly in[39,40]. At fixed values of E and p, the length of the gap was varied and the distribution of $|\ln(n/n_0)| = f(t)$ was plotted. In view of the increasing statistical scatter with respect to the time τ with decreasing gap length, what was determined in these experiments was the average statistical time τ_{st} in the distribution $|\ln(n/n_0)| = f(t)$ under the condition $|\ln(n/n_0)| = 1$. Figure 6 shows plots of τ_{st} against the gap length d for aluminum electrodes. Each such plot has three characteristic sections: a region of slow variation of τ_{st}, an inflection region, and a region of rapid growth of τ_{st} with decreasing d. It should be borne in mind that the change of the time τ_{st} is governed only by processes of discharge formation. The current of the electrons initiating the breakdown remained unchanged during the plotting of $\tau_{st}(d)$, since E, p and the cathode surface were unchanged. The latter was monitored by comparing the two distributions $|\ln(n/n_0)| = f(t)$ before and after plotting the $\tau_{st}(d)$ curve.

It was found in[35] that in the case of copper and tungsten electrodes the time τ_{st} increases rapidly with increasing number of prior discharges. It is shown in[41] that this is due to a deterioration of the photoemissive properties of the cathode and explains the presence of several maxima in the distribution of the delay time of a nanosecond discharge, observed in[42], since, as shown in[15,35], the photoemissive properties of the cathode varied during the course of accumulation of the statistics. These facts demonstrate the important role played by the photoeffect on the cathode in the secondary process.

It is suggested in[15] that the growth of the gap current during the initial stage of the discharge is due to the development of avalanche chains. Such chains can be produced when the field expels some of the electrons from the preceding avalanche and the succeeding avalanche is formed, when the gas ahead of the avalanche becomes photoionized, or else as a result of the "runaway" electrons. Owing to the low conductivity of the avalanche chains, their number must be large to pass a large current.

The development of a discharge was analyzed in[43] with allowance for the development of avalanche chains and the photoemission of electrons from the cathode. A simplified model of the avalanche chain was used, according to which the avalanche grew exponentially to the critical size within a time t_c, and the number of electrons remained unchanged after the critical value N_c was reached. It was also assumed that the current of the circuit was due only to the electrons of the leading avalanche, with $d \gg x_c$ at all times. The expression obtained for the characteristic formation time of a discharge in which the current in the gap is $i = i_c$ is

$$\tau = \left(\frac{e\tau_{exc}}{16\pi\varepsilon_0 v_a u_T \gamma}\right)^{1/2} \ln\left[\left(\frac{i_c \alpha d}{2i_0}\right)\left(\frac{\gamma e}{\pi e_0 u_T v_a \tau_{exc}}\right)^{1/2}\right], \qquad (12)$$

where e is the electron charge, ϵ_0 is the dielectric constant, u_T is the thermal energy of the electron in the avalanche in eV, γ is the number of secondary electrons produced on the cathode as the result of the photoeffect in a single ionization act in the avalanche chain, τ_{exc} is the average time of emission of the excited gas molecules, i_0 is the current of the initiating electrons, and v_a is the velocity of the avalanche circuit.

As already shown in Sec. (b), the time τ increases strongly with increasing d in gaps of length $d < d_0$, and changes little with d when $d > d_0$. If it is assumed that a gap $d = d_0$ corresponds to the condition that part of the avalanche chains touch the anode after a time τ, then at $d > d_0$ the current $i = i_c$ is reached within that time even before the avalanche chains touch the anode. Therefore the time τ should not depend on d. This is confirmed by formula (12), since the length of the gap d is under the logarithm sign and has practically no influence on the time τ. It also follows from this assumption that

$$d_0 = v_a \tau. \qquad (13)$$

At a fixed pressure, the velocity is $v_a \sim v_- \sim E^{1/2}$ and the electron thermal energy is $u_T \sim E^{2/3}$.[8] For a discharge in an air gap between copper electrodes[13] we have $\gamma \sim E^{1.8}$. Consequently, according to (12) and (13),

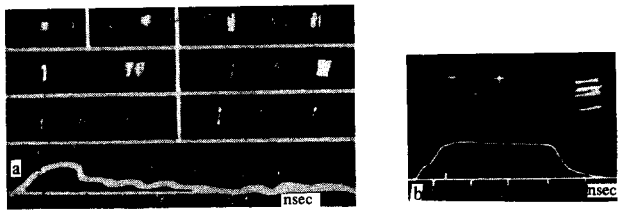

FIG. 7. Development of discharge initiated by a small number of electrons.

$\tau \sim E^{-3/2}$ and $d_0 \sim E^{-1}$, which is in satisfactory agreement with the experimental plots of $\tau(E)$ (see Fig. 5).

Electron-optical investigations of the structure of the discharge space in air at a pressure ~50 Torr were carried out in[44] without irradiating the cathode from any source. During the stages of discharge formation and of the start of the current growth, three-dimensional glow in several narrow channels were observed. Such investigations were carried out in[45] with air at atmospheric pressure and at an electric field intensity E = 80 kV/cm in gaps 4 and 2 mm long. The discharge was investigated during the first few nanoseconds after the application of the pulse. The results of[45] have shown that after a voltage is applied to the gap, three-dimensional glow is observed at the cathode, which subsequently propagates to the anode at a velocity $\sim 10^8$ cm/sec and grows simultaneously in diameter.

Figure 7a shows image-converter diagrams of the glow and an oscillogram of the discharge development in air at E = 100 kV/cm (p = 760 mm Hg, d = 0.6 cm)[46,47]. The cathode was irradiated by an auxiliary spark simultaneously with the application of the high-voltage pulse. The oscillogram shows sections of rapid and slow voltage fall-off. It is seen from the image-converter diagrams that individual diffuse channels appear in the gap 1–2 nsec after the rapid voltage fall-off; after a certain time, bright formations appear in individual spots of the diffuse channels. In the course of time, a contracted channel is produced in the gap.

Investigations by the method of interrupted discharge[48] have also confirmed that when the cathode irradiation intensity is decreased the discharge-formation time increases, but the duration of the slow voltage fall-off is then decreased, owing to the formation of individual channels. Figure 7b shows a photograph of the glow in the gap, obtained by the interrupted-discharge method, and reveals that one or several narrow channels are already present in the gap at the instant when the fall-off sets in. The number of such channels can exceed 10. Such channels are described also in[42,49]. The cause of these channels has not yet been completely established. It can be assumed that they are connected with the uneven distribution of the initiating electrons on the cathode, owing to the presence of electron-emitting centers on the cathode surface. In this case, each channel should correspond to a separate emission center.

It was shown in[50] that in the case of a small number of initiating electrons the current and voltage of the spark during the stage of rapid growth of the current are satisfactorily described by the avalanche-theory formulas obtained for multielectron initiation (see Chap. 4, Sec. a)). The reason is that the fall-off of the gap voltage occurs within the time of one avalanche generation after a large number of electron avalanches is accumulated.

It was noted in[48] that in some cases there is no stage of slow voltage fall-off, even though the maximum rate of fall-off remains the same as the calculated one (see formula (23) below). This is apparently due to the fact that the growth of the current in the gap is the result of rapid ionization of the channels that intersect the diffusion volume (see Fig. 7).

4. PULSE DISCHARGE INITIATED IN A GAS BY A LARGE NUMBER OF INITIAL ELECTRONS

a) **Experimental results.** An investigation of the influence of the number of initiating electrons on a pulsed nanosecond discharge in air at atmospheric pressure, at gap lengths up to 6 mm and at electric field intensities up to 10^5 V/cm, was carried out by Fletcher[37]. He used a microoscillograph and high-speed circuits with 10^{-10} sec resolution, and also a pulse generator with a rise time 3×10^{-10} sec.

The cathode was illuminated 60 nsec prior to the arrival of the voltage pulse on the gap, and the photocurrent from the cathode, in the absence of a time-delay spread, was 1.7×10^{-8} A. Inasmuch as at overvoltages >80% each electron released from the cathode is effective in the sense of breakdown initiation[21], it follows that about 10^4 electrons are accumulated prior to the arrival of the pulse at the cathode, and this eliminates completely the statistical spread of the discharge-delay time. The delay time was taken in[37] to be equal to the discharge formation time τ. The dependence of τ on the field intensity E at atmospheric pressure in air is shown in Fig. 5 (curve 1). The value of E was regulated by varying the length of the gap d at a fixed voltage-pulse amplitude E_0. At $E \geq 50$ kV/cm, the value of τ depends only on the field E and does not depend separately on the amplitude of the voltage and on the length of the gap. At $E < 50$ kV/cm, the experimental points at the voltage $U_0 = 7.5$ kV correspond to larger formation times in comparison with points pertaining to higher voltages. At $E < 42$ kV, the curve for $U_0 = 12.7$ kV lies above the curve for $U_0 = 18$ kV.

The function $\tau(E)$ was determined in[36] for single-electron and multielectron initiation. To apply ultraviolet radiation to the cathode, a hole was drilled in the anode and covered with a grid. A diaphragm and quartz glass were installed between the grid and the spark illuminating the cathode. The quartz glass is necessary to filter out the short waves and to prevent photoionization of the gas. The current of the electrons initiating the discharge was regulated by the size of the diaphragm and by the length of time between the arrival of the ultraviolet flash and the voltage pulse. These experiments confirmed the conclusion that when the number of initial initiating electrons is of the order of 10^4, there is no spread in the discharge delay time, and the $\tau(E)$ dependence agrees with that obtained in[37].

Figure 8 shows the experimental curves (solid) obtained in[37] for the relative gap-voltage fall-off following a breakdown in air, for different gap lengths d and

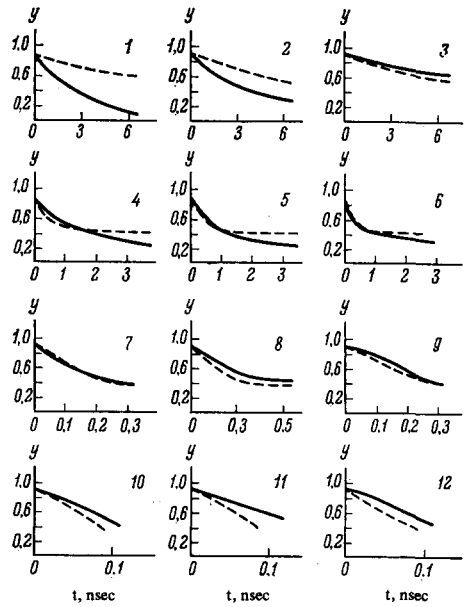

FIG. 8. Discharge-gap voltage fall-off. The respective values of E_0 (kV/cm) and d (mm) for the curves are as follows: 1–46.1 and 2.74; 2–46.1 and 3.91; 3–45.9 and 1.53; 4–66 and 2.18; 5–64.6 and 1.68; 6–66.4 and 1.37; 7–84.4 and 2.13; 8–78.2 and 1.83; 9–79.2 and 1.37; 10–107.4 and 1.67; 11–104.4 and 1.37; 12–101.8 and 1.07.

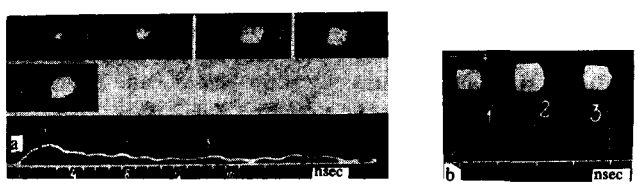

FIG. 9. Development of discharge following multielectron initiation.

for different electric-field intensities E_0 (the dashed curves were calculated in[50]).

Electron-optical frame-by-frame photography of the glow of a discharge in atmospheric air at E = 55–100 kV/cm, with exposure of 3 nsec[51], was performed in[46]. Figure 9a shows the image-converter pictures of the glow of a discharge developing in a gap 6 mm long at a field intensity 100 kV/cm (p = 760 mm Hg). The cathode was irradiated with an ultraviolet flash from a spark 10^{-8} sec prior to the arrival of the pulse at the gap. The gap-voltage fall-off first proceeds rapidly and then slows down. The image-converter pictures show that uniform diffuse glow is produced in the gap already during the first nanosecond after the application of the voltage pulse, and the glow intensity increases rapidly during the stage of the rapid voltage fall-off. For 15 nsec after the start of the voltage fall-off, a uniform diffuse glow remains in the gap. The glow of the gap during different stages of discharge development in air at atmospheric pressure, at gap lengths 3–6 mm and at E/p = 90–100 V/cm-mm Hg, was observed also by the interrupted-discharge method. Single rectangular pulses were used, with amplitude up to 45 kV and with a regulated pulse duration from 5 to 20 nsec. The surface of the cathode was irradiated by a corona-producing needle located in the immediate vicinity of the cathode. The pulse oscillogram and the corresponding glow in the gap during the discharge development, obtained by the interrupted-discharge method, are shown in Fig. 9b. A characteristic feature of the nanosecond-pulse discharge is the absence of a contracted channel at high gas pressure for a prolonged time (up to 20 nsec) after the start of the increase in the current. The discharge current reaches several hundred amperes in this case.

It was assumed in[37] that the discharge is initiated by a single electron and not by 10^4 electrons. This contradiction was first pointed out in[42]. It was assumed that the $\tau(E)$ dependence obtained in[37] agrees with the deductions of the streamer theory and with Raether's breakdown criterion (cf.[2,3]). The latter states that the time τ is determined mainly by the time necessary for the avalanche to grow to a size at which it goes over into a streamer. Since a streamer develops much more rapidly than an avalanche, the influence of its development time on τ can be neglected. Raether[3] has established that an avalanche goes over into a streamer when the number of electrons in the avalanche is of the order of 10^8. $\tau(E)$ was calculated in[37] with allowance for the influence of the avalanche space-charge field, and it was found that

$$\tau = \ln N_c/\alpha v_-, \qquad (14)$$

where N_c is the critical number of the electrons in the avalanche and depends in a complicated manner on the field intensity E, the gas pressure p, and the type of gas. However, as noted in[37], the result changes little if N_c changes appreciably, since N_c is under the logarithm sign in (14). The dependence of N_c on p and E can therefore be neglected, with good approximation, and one can put $N_c = (1-5) \times 10^8$. Then $\tau \approx 20/\alpha v_-$, thus describing satisfactorily the $\tau(E)$ curve shown in Fig. 5.

It was established in[52] that a $\tau(E)$ dependence similar to that in[37] can be obtained by forgoing the streamer theory and regarding the discharge-formation process as simply the development of an electron avalanche. If it is assumed that the avalanche can grow to a size capable of ensuring a large current in the gap and a fall-off in its voltage as a result of the decrease in the voltage across the main resistance of the circuit, then the calculated current-growth time is in good agreement with the experimentally measured value[37].

It was assumed in[52] a gap current up to about 100 amperes can result from the development of a single electron avalanche. At a gap length on the order of 1 mm and an avalanche drift velocity $v_- = 10^7$ cm/sec, this yields $\sim 10^{13}$ electrons in the avalanche. The possibility that an electron avalanche grows to such a value is confirmed by the calculations given in Chap. 2 and by the experimental data of[19,20]. As shown above, when the number of electrons in the avalanche is of the order of 10^8 (for E/p ≈ 40 V/cm-mm Hg), the influence of the space-charge field of the ions is so large that the growth of the number of electrons ceases to be exponential and becomes slower. At large values of E/p, this effect of slowing down of the avalanches takes place at even a smaller number of electrons in the avalanche (see Fig. 3).

To explain the $\tau(E)$ dependence obtained in[37], it was proposed in[53] to use the diffusion theory developed

for a microwave discharge. However, only the terms responsible for impact ionization and for the trapping of the electrons were retained in[53] in the continuity equation for the electrons, and diffusion was neglected. It was assumed in[53] that the breakdown sets in when a definite ratio of final to initial electron density n_{fin}/n_0 is attained in the gap. Then

$$\tau = \ln (n_{fin} n_0^{-1})/(\alpha - \eta)\, v_-, \qquad (15)$$

where η is the electron trapping coefficient. Since $\alpha \gg \eta$ for air at atmospheric pressure, and a value $n_{fin}/n_0 = 10^8$ was chosen in[53] without any justification whatever, it was natural for the $\tau(E)$ dependence given by (15) to agree fully with (14) and with the experimental results obtained in[37].

b) **Theory of avalanche-like growth of current in a discharge initiated by many electrons.** To explain the experimentally obtained[37] $\tau(E)$ dependence, it was assumed in[36] for the first time that the discharge is initiated not by a single electron, but by many of them (on the order of 10^4). In the same paper, we introduced the concept of multielectron and single-electron discharge initiation and showed that for the same electric field E the value of τ is much lower in the former case than in the latter.

Assume that the gap current grows as the result of avalanche multiplication of N_0 initiating electrons. To calculate the time dependence of the spark current i(t), we examine the transient process in a circuit consisting of a voltage source U_0, a resistance, and a spark gap with interelectrode capacitance. This is equivalent to a circuit in which the spark gap is connected in series with a coaxial line, as in the experiments of[36,37]. The spark gap is replaced by a current generator. The equations for the current takes the form

$$C\,(dU/dt) + N_0 e v_- d^{-1} \exp\left(\int_0^t \alpha v_-\, dt\right) = i\,(t), \qquad i\,(t) = (u_0 - u)/R, \qquad (16)$$

where e is the electron charge, U_0 the pulse amplitude, v_- and α the electron drift velocity and the impact-ionization coefficient, C the interelectrode capacitance, R the circuit resistance, and U the gap voltage.

The discharge formation time τ is determined from the current oscillograms and is measured from the instant of voltage application to the instant when the current reaches a certain value i_C determined by the resolution of the oscilloscope tube. Since a weak current flows through the gap during the time τ, we have $Ri_C \ll U_0$ and we can assume that α and v_- are constants. Then

$$\tau = (\alpha v_-)^{-1} \ln [i_C d\,(1 + RC\alpha v_-)/eN_0 v_-]. \qquad (17)$$

If we assume that the current i_C is ~5% of U_0/R, then we can show that for the experimental conditions of[37] the quantity under the logarithm sign is of the order of 10^8. This agrees well with the value of N_C in (14). Since i_C is under the logarithm sign, a certain leeway in the choice of i_C is justified, because an error in i_C by even one order of magnitude makes the error in τ only 10–15%. Consequently, formula (17) for the dependence of τ on the electric field E and on the gas

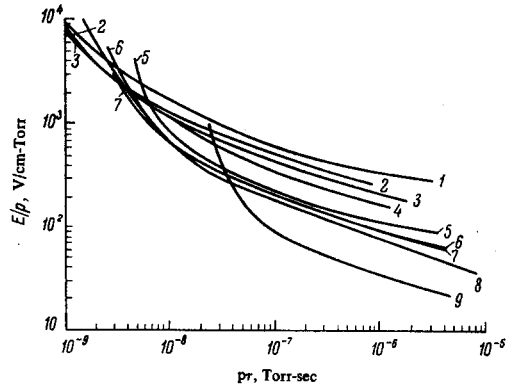

FIG. 10. Experimental [53] breakdown-formation time for different gases: 1–freon-C318; 2–freon-114; 3–freon-12; 4–SF_6; 5–N_2; 6–air; 7–O_2; 8–Ar; 9–He.

pressure p is in good agreement with the results of experiment, just as (14).

It follows from (14) and (17) that the $\tau(E)$ dependence can be written in a form that agrees with the similarity law. Indeed, since $\alpha/p = f_1(E/p)$, $v_- = f_2(E/p)$, and furthermore τ depends little on i_C, it follows that

$$p\tau = F\,(E/p). \qquad (18)$$

The validity of (18) for many gases was demonstrated in[53], where the voltage range from 4 to 30 kV, the pressure from 1 to 760 mm Hg, the gap length from 0.1 to 6 cm, and the obtained τ was 0.5–30 nsec. The dependence of $p\tau$ on E/p for different gases is shown in Fig. 10.

Formula (17) describes correctly the dependence of τ on E/p and agrees with the similarity law only if a total avalanche current equal to or larger than i_C can be obtained over the length of the gap. If such a current cannot be obtained, formula (17) ceases to be valid and one should expect deviation from the similarity law. The condition under which such a deviation is to be expected takes the form $d < \tau v_-$. At $RC\alpha v_- < 1$, it takes the form

$$d < \alpha^{-1} \ln (i_C d/eN_0 v_-). \qquad (19)$$

To make a comparison of (19) with experiment convenient, we multiply the left- and right-hand sides by E_0 and compare the results with the experimental data[37]. We then obtain

$$U < (E/\alpha) \ln (i_C d/eN_0 v_-). \qquad (20)$$

If we substitute in (20) the value of α from (2), then the value of E/p below which the similarity law ceases to be satisfied is given from the relation

$$E/p = B_0\,\{1 + (M/2U_0) + [MU_0^{-1} + (M^2/4U_0^2)]^{1/2}\}, \qquad (21)$$

where $M = (1/AB_0) \ln (i_C d/eN_0 v_-)$. At $U_0 = 12.7$ and 7.5 kV and at p = 760 mm Hg, the values of the electric field E in accordance with formula (21) are 42 and 51 kV/cm, respectively. The experimental values of E (see Fig. 5) are 42 and 50 kV/cm[37].

It was shown in[50] that the stage of rapid gap-current growth can be attributed, just as the stage of discharge formation, to the development of electron avalanches with allowance for the variation of the gap

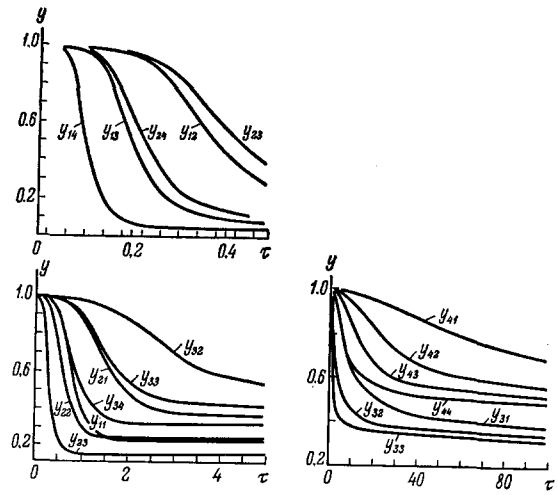

FIG. 11. Plot of $y(\tau)$ for a = 160, 130, 90, and 60 V/cm-mm Hg and b = (2, 5, 10, and 20) × 10^{-4} (mm Hg)^3 cm^3/v^2.

voltage as a result of the presence of an active resistance in the discharge circuit.

In the presence of an interelectrode capacitance C, Eq. (16) with an allowance for the relation (3′) for v_- takes the form[50]

$$\ddot{y}\dot{y} + y(1-\dot{y}) + b(1-y-\dot{y})\psi(ay) = 0, \qquad (22)$$

where $y = E/E_0 = U/U_0$, $\dot{y} = dy/d\tau$, $\ddot{y} = d^2y/d\tau^2$ ($\tau = t/\theta$, and $\theta = RC$); $\psi(ay) = (E/p)^2\alpha/p$, $\alpha = E_0/p$; $b = p^2C_0\theta/E_0$, E is the field intensity in the gap, and $E_0 = E_0/d$ is the field intensity at which breakdown of the gap takes place. Equation (22) for air gaps was solved numerically with an M-20 computer. The result of the calculations are shown in Fig. 11 (the first subscript of y corresponds to the number a, and the second to b). The voltage fall-off curve is at first steep and then slows down. The transition from the rapid current growth to the slow one is due to the increase of the voltage drop on the active resistance with increasing current. This decreases the field intensity in the gap and accordingly decreases the impact-ionization coefficient α and the electron drift velocity v_-.

It follows from (22) that the voltage and current of the spark do not depend on the number of initial electrons N_0. Figure 8 shows the experimental[37] (solid curves) time dependence of the gap voltage and those calculated with the avalanche model (dashed curves) at different values of E_0/t. It follows from Fig. 8 that wherever the similarity law holds for the time τ ($E_0/p \geq 66$ V/cm-mm Hg) the experimental and theoretical time dependences of the gap voltage are in satisfactory agreement. At $E_0 > 130$ kV/cm, the theoretical curves lie lower than the experimental ones. This is attributed to the small value of the time τ, which amounts to 0.2 nsec and is almost equal to the transient time constant of the recording system[37,54].

At an interelectrode capacitance C = 0, and also when α/p is approximated by formula (2) in the range $40 < E/p < 140$ V/cm-mm Hg, we obtain from (22)

$$dz/d\tau = (1-z)^2(z-D)^2 z,$$

where

$$D = 1 - (B_0/E_0p^{-1}), \quad \tau = t/\theta_1, \quad \theta_1 = (AC_0p)^{-1}(E_0/p)^{-3},$$
$$z = i/U_0R^- = 1 - (E/p)/(E_0/p) = 1 - y.$$

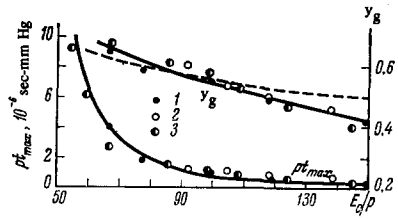

FIG. 12

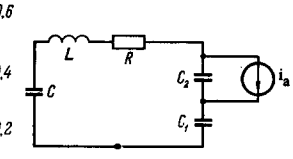

FIG. 13

FIG. 12. Experimental (upper curve) and theoretical (dashed curve) values of $y_g = E_g/U_0$ and theoretical value of pt_{max} (lower curve) vs. E_0/p.

FIG. 13. Equivalent circuit of a discharge of a capacitor into a gas gap with a dielectric-coated electrode.

The slope di/dt assumes a maximum value $(di/dt)_{max}$ on the steep section of the z(t) curve. The maximum slope of the current in the gap is best characterized by a time $t_{max} = I_0(di/dt)^{-1}_{max}$, where $i_0 = U_0/R$. The time t_{max} satisfies the similarity law, and therefore

$$pt_{max} = (E_0/p)^{-3}/AC_0\,(dz/d\tau)_{max}. \qquad (23)$$

The dependence of pt_{max} on E_0/p, plotted in accordance with formula (23), is shown in Fig. 12, together with the experimental values (circles) obtained for pt_{max} in[37]. In this experiment, the diameter of the flat electrodes was chosen such as to be able to neglect the effect of the interelectrode capacitance on the value of t_{max}[50]. The spark current and voltage first vary rapidly, and then slow down because of the decrease of α and v_-. The gap voltage at which the slope of the voltage fall-off is much smaller than the maximum value can be calculated theoretically when solving (16). Figure 12 shows the relative gap voltage $y_g = U_g/U_0$ at which the rate of current growth decreases to one-fifth the maximum value[50], as a function of E_0/p. The same figure shows the experimental plot of $y_g(E_0/p)$ for air at atmospheric pressure and for gap lengths d = 1 (curve 1), 2 (2), and 4 mm (3)[50].

In the foregoing analysis of the discharge, the parameters characterizing the properties of the electrodes do not enter in the derived formulas. It is therefore of interest to analyze the development of a discharge in the presence of a dielectric on the electrodes. If the dielectric surface is assumed to be equipotential, then the gap can be regarded as consisting of a gas section, a dielectric section, and sections with appropriate capacitances. The current through the gas section is determined in analogy with (16). It is easy to show that for this case

$$\tau = (\alpha v_-)^{-1} \ln [i_c d_2 (1 + \alpha v_- RC_3)/eN_0 v_-], \qquad (24)$$

where $C_3 = C_1C_2/(C_1 + C_2)$, C_1 is the capacitance of the dielectric layer on the electrodes, and C_2 and d_2 are the capacitance and length of the air gap. If $C_1 \gg C_2$, then formula (24) goes over into (17), i.e., the presence of a dielectric film on the electrodes does not influence the value of the time τ, as was indeed observed in[37,55].

It was proposed in[56] to generate nano- and subnanosecond large-current pulses by using a discharge between electrodes of a dielectric with large ϵ and multielectron initiation. The equivalent circuit for the discharge of a capacitance C into a gap with a die-

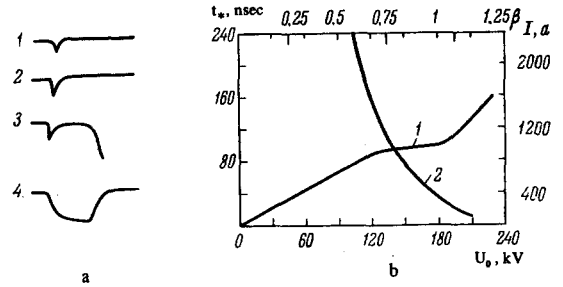

FIG. 14. a) Current oscillograms of a discharge with a beam; b) experimental plots.

lectric is shown in Fig. 13. The value of i_c is determined by the second term of (16). The influence of the inductance L or of the resistance of the discharge circuit on the current is significant when $Li_a/t_p \sim U_0$ or $Ri_a \sim U_0$. Assuming $C_1 \gg C \gg C_2$ and disregarding R and L, the result obtained in[56] was

$$i_a = \alpha_0 v_0 U_0 CF(E_0/p), \quad t_p = U_0 C/i_a,$$

where $F(E_0/p) \approx 0.1 + 5 \cdot 10^{-4}[(E_0/p) - 100)]$, $100 < E/p < 400$ V/cm-Torr, t_p is the duration of the current pulse, i_a is the pulse amplitude, and u_0, α_0, and v_0 are the initial values of the voltage, impact-ionization coefficient, and drift velocity. It is possible in this case to eliminate the localization of the discharge current in a channel and thereby eliminate the influence of its inductance on the duration and amplitude of the current pulse.

c) **Discharge in a gas in the presence of an intense source of preliminary ionization.** The theory of avalanche switching with multielectron initiation, described in Chap. 4b, can be extended not only to gaps with over voltages, but also to the case when the breakdown occurs at the static breakdown voltage or at lower voltages. The main requirement is to ensure an initiating-electron current $i_0 = eN_0 v_-/d$ such that at a gas gain $\leq 10^8$ of the discharge current in the circuit reaches a value at which the gap voltage begins to fall off. Then, if the initiating electrons are distributed over the cathode surface, the breakdown is initiated by ionization in the gas volume without formation of localized spark channels. For example, at an initiating-electron current $i_0 \sim 10^{-7}$ A, i.e., at $N_0 \sim 10^5$ and at a gas gain 10^8, the current in the external circuit reaches ~10 A. Recognizing that additional photoelectrons will come from the cathode as a result of the photoeffect during the time that the avalanche grows to $N = 10^8$ electrons, it becomes obvious that the total discharge current greatly exceeds 10 A. Such a discharge is realized by initiation with an intense ultraviolet flash, as was used, e.g., in[57]. The ultraviolet radiation incident on the cathode produces a large number of electrons as the result of the photoeffect. It is shown in[57] that as the air-gap voltage reaches the static breakdown value, the time between the instant of the appearance of the flash and the breakdown approaches the time d/v_- required for the avalanche to traverse the gap. It is easy to show that this result can be obtained by starting from the theory developed in Chap. 4b.

If we replace α in formula (17) for the time required for the gap current to grow to the value i_c, which can be regarded as the breakdown time, by the value $\alpha \approx 20/d$ obtained from Raether's condition for static breakdown[1,2] i.e., if we assume that the gas gain does not exceed 10^8, then we obtain

$$\tau = (d/v_-) \ln (i_c d/eN_0 v_-)/20 \approx d/v_-.$$

The breakdown formation time τ was calculated in[58] for the case when short-duration ($\sim 10^{-9}$ sec) ultraviolet flashes were used to irradiate gaps with voltages amounting to 90--95% of the static breakdown value. It was found that the time τ lies in the interval $d/v_- < \tau \ll d/v_+$, where v_+ is the drift velocity of the positive ions. A strong dependence of τ on the value of the undervoltage was obtained.

To eliminate the discharge channel in a high-pressure gas, it was proposed in[56] to initiate the discharge by a beam of fast electrons. An electron beam with cross section 20 cm^2 was introduced through a tantalum foil into a nitrogen-filled gap into which a line with wave resistance $R = 10\ \Omega$ was discharged[59]. The line was charged by pulse to a voltage $U_0 = 5$--250 kV. The maximum beam energy was 180 keV and the average was ~80 keV. Typical discharge current oscillograms are shown in Fig. 14a. At $U_0 \geq U_*$ (U_* is the static breakdown voltage), the discharge current I is similar in shape to the beam current i_- (curves 1 and 2 of Fig. 14a), and increases linearly with i_- (curve 1 of Fig. 14b). At $U_0 \geq U_*$ and $p \gg 3$ atm, the discharge current increases sharply in a time t_* after the appearance of the beam (Fig. 14a, curve 3); at $U_0 < U_*$ and $p \sim 1$ atm, the current begins to grow immediately without any delay whatever (curve 4 of Fig. 14a). In this case, as in all cases when $U_0 < U_*$, glow was observed in the entire volume of the gap, whereas at $U_0 > U_*$ and $p \geq 3$ atm, a spark channel was observed in the gas gap at $t > t_*$. Typical experimental plots of $t_*(U_0)$ (2) and $I(U_0)$ (1) are shown in Fig. 14b. In the figure, $\beta = U_0/U_*$.

For the line at $v_- t \ll d$, the discharge current is[59]

$$i = U_0 \lambda t/(1 + R\lambda t), \tag{25}$$

where $\lambda = n_0 k_0 \langle\sigma\rangle i_-/pd$, $n_0 = 3.5 \cdot 10^{16}$ cm^{-3} is the concentration of the gas molecules at a pressure of 1 mm Hg, $\langle\sigma\rangle$ is the average cross section for gas ionization by the electron beam, k_0 is the coefficient of proportionality between the drift velocity and the quantity U_0/pd, and d is the gap length. The influence exerted by the uneven potential distribution along the gap on the current can be taken into account by solving the one-dimensional Poisson equation and the continuity equation, using successive approximations. It can be shown that at $v_- t \ll d$ the cathode drop is

$$U_c \approx U_0 \cdot 2v_- t/d.$$

The linear initial section of the $I(U_0)$ curve (I is the current amplitude) (curve 1, Fig. 14b) is the well accounted for by formula (25). The saturation at $U_0 \leq U_*$ is due to the growth of the cathode voltage drop U_c and the decrease of the voltage drop in the discharge column. The growth of $I(U_0)$ at $U_0 > U_*$ is due to the avalanche multiplication of the electrons. In the latter case, the discharge current was independent of

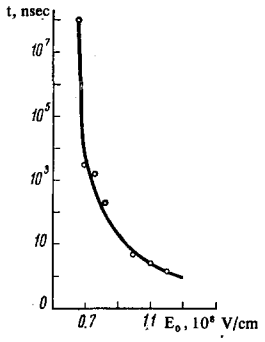

FIG. 15

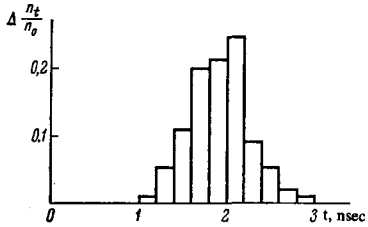

FIG. 16

FIG. 15. Time prior to the disintegration of a sharp point in vacuum vs. the applied field E_0 [62].

FIG. 16. Distribution of delay time t_d.

the initial number of electrons, as follows from the conclusions of Chap. 4b. At $U_0 > U_*$, the current $I(U_0)$ in the experiment[59] reached a maximum at a certain time after the vanishing of the beam current i_-. At $U_0 < U_*$, to the contrary, the maximum of the current $I(U_0)$ occurred practically exactly at the same time as the trailing edge of the i_- pulse. It was shown relatively recently that the space charge in a gas can be used to pump gas lasers operating at high gas pressures[60]. An important role is played in the pumping process by the energy absorbed by the gas-discharge plasma from the storage device (capacitor or long line). It is easy to show that in the case when the impedances of the discharge gap and the surge element are equal, practically the entire energy of the latter is absorbed by the plasma within the time necessary for the pulse to traverse double the line length. In the case of avalanche multiplication of the electrons, according to the calculation curves (see Fig. 11), the resistance of the discharge gap can be made commensurate with the wave resistance of the line on the flat sections of the $y(\tau)$ curves. This makes it possible to determine the relation between the parameters of the gas discharge and the parameters of the external circuit and thus obtain optimal pumping conditions. If there is no avalanche multiplication, when $U_0 \ll U_*$, such a relation is easily obtained from (25). In[59], the specific energy dissipated in the gap following the discharge of a long line charged to 700 kV, at a current 40 kA, was approximately 10 J/cm^3.

5. FEATURES OF DISCHARGE IN GAS IN AN ULTRASTRONG ELECTRIC FIELD

As already noted, the surfaces of real electrodes always have microscopic projections at which the electric field can be stronger by hundreds of times. In a strong electric field, the field-emission current from the projections becomes so strong that the projections explode and form a plasma that leads to further enhancement of the electron emission from the cathode[61].

An experimental investigation of the explosion of sharp-point electrodes in vacuum following application of rectangular pulses of duration $t_p = 5 \times 10^{-9}$—4×10^{-6} sec is described in[62]. At $t_p = 5 \times 10^{-9}$ sec, a current density exceeding 10^9 A/cm^2 could be obtained from an emitter of radius $r_e \approx 10^{-5}$ cm with a cone angle $\theta \approx 15°$. The time t elapsed before the disintegration of the projection was found to be strongly dependent on the field E_0 at the point (Fig. 15).

It was shown in[62] that the explosion of microscopic projections on the surface of the cathode initiates an electric discharge in vacuum. In the case of breakdown of gas-filled gaps with field intensity up to 10^6 V/cm, the explosion of the microscopic projections can exert a very strong influence on the discharge process. The delay time of the breakdown, at an average electric intensity 10^6 V/cm between flat electrodes, is therefore 10^{-9} sec.

An investigation of pulsed breakdown of air gaps at atmospheric pressure and at an electric field intensity $(0.3—1.4) \times 10^6$ V/cm was carried out in[35]. The pulse-front duration was 0.3 nsec. The breakdown delay time t_d was assumed to be the time from the start of the application of the voltage to the start of the rapid growth of the current. Since t_d had a statistical scatter, the statistical distribution of this time was determined. The values of t_d depended on the cathode material, on the degree of its surface finish, and on the prior conditioning. Figure 16 shows the distribution of the times t_d at E = 1.4 times 10^6 V/cm and a gap length 0.1 mm, for highly polished copper electrodes (p = 760 mm Hg). The plots of the logarithm of the relative number of breakdowns n/n_0 (n_0 is the total number of breakdowns having a delay time t_d and longer) against this time were similar. At large t, these plots are straight lines, and at small ones they have bends. The slopes of these lines depend on the field intensity and on the gas pressure.

An investigation of the time of current growth and of the spark voltage fall-off in ultrastrong fields is made difficult by the shortness of this time. It does not exceed 10^{-10} sec. A step-like voltage fall-off was observed in[39] at $E/p = 10^3$—10^4 V/cm-mm Hg and at air pressure 1—10 mm Hg, the voltage-step duration being of the order of 10^{-8} sec.

Attention was called in[33,34] to the role of the "runaway" electrons in a discharge plasma. In a nanosecond pulsed discharge, the degree of ionization of the plasma is close to that in an avalanche of critical size. According to the data given in Chap. 2, the degree of ionization in nitrogen at a pressure p = 760 mm Hg and E = 10^5 V/cm, was 10^{-5} after $\sim 10^{-9}$ sec. For avalanches at pressures lower than atmospheric, this value is even lower[3]. At such values of the degree of ionization, the collision between the electrons and the ions can be neglected in the energy balance of the electrons, and it is necessary to take into account only the collisions of the electrons with the gas molecules; at an electron energy $W \geq 5eU_i/2$, this leads to the equation[63]

$$dW/dx = eE - (2\pi e^4 nz/W) \ln (2W/\bar{\epsilon}), \qquad (26)$$

where U_i is the ionization potential, $W = mv^2/2$; m, v, and e are respectively the energy, mass, velocity, and charge of the electron, z is the total number of electrons in the molecule, x is the path of the electron along the field line, $\bar{\epsilon}$ is the averaged excitation energy of the electrons contained in the molecule, and n is the

gas density. It follows from (26) that at $W = 2.72\bar{\epsilon}$ the second term is maximal. Then

$$E = E_c = 4\pi e^3 nz/2.72\bar{\epsilon}, \quad (27)$$

and $dW/dx = 0$.

If $E > E_c$, then $dW/dx > 0$ and the electrons in the discharge plasma begin to be accelerated continuously. E_c is called the critical field of electron "runaway." It follows from (27) that $E_c/p = 3390z/\bar{\epsilon}$, where $\bar{\epsilon}$ is the energy in eV, E_c is in V/cm, and p is in mm Hg. For nitrogen, $z = 14$, $\bar{\epsilon} \approx 130$ eV[64], and $E_c/p \approx 365$ V/cm-mm Hg.

The integral (26) shows that at $E/E_c \geq 2$ and for $2Ede/\bar{\epsilon} > 100$ (where d is the gap length) the energy of an electron "running away" from the cathode region approaches $W \approx eEd$ at the anode; this should cause x-rays to be emitted from the anode.

X-radiation from a discharge in helium at atmospheric pressure between a pointed cathode and a flat anode was observed in[65]. The voltage pulse duration was 10 nsec and the amplitude was 240 kV. The measured energy of the x-ray quanta was 10--13 keV and the number of accelerated electrons was of the order of 10^{11}. No x-radiation was registered in[66] for a discharge in air under analogous conditions.

X-radiation in air at atmospheric pressure was observed in[33] at a gap length 0.4 mm and a field intensity 1.3×10^6 V/cm; the amplitude of the pulse applied to the chamber was 52 kV and the rise time was 1 nsec. Under these conditions, the quantum energy was ~20 keV.

The dependence of the x-ray intensity on E/p was investigated in[66]. The electric field in the gap was uniform and the field rise time was 1 nsec. The field intensity was ~100 kV/cm and the gap length 4 mm. The air pressure was varied in the range from 80 to 760 mm Hg. The anode was an aluminum plate 0.5 mm thick, on which a scintillator was placed; the scintillator glow was registered with a photomultiplier.

Plots of the x-ray intensity against E/p are shown for air and helium in Fig. 17 (the intensity was measured after passage through an aluminum anode 0.5 mm thick within a solid angle 0.2π). It follows from the figure that in air the intensity decreases sharply with increasing pressure, whereas in the case of helium it remains appreciable even at p = 760 mm Hg.

The x-ray quantum energy was measured in air at p = 80 mm Hg and in helium at p = 400 mm Hg by the foil method. It was shown that for discharge in air at p = 80 mm Hg, gap length 0.4 cm, and voltage 40 kV between the electrodes the maximum x-ray quantum energy was 16 keV. If it is assumed that the radiation is produced by electrons of energy 16 keV, then simple calculations show that a discharge in air at a pressure 80 mm Hg contains $\sim 5 \times 10^{10}$ electrons having this energy.

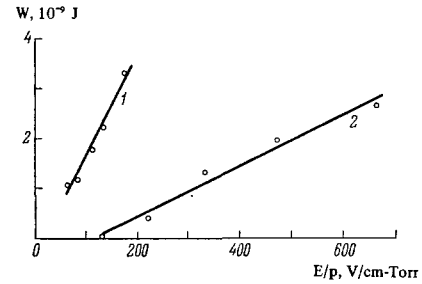

FIG. 17. X-ray energy per pulse vs. E/p in helium (1) and in air (2).

6. CONCLUSION

We have considered a pulsed electric discharge in gases at appreciable gap overvoltages, when the characteristic time of discharge development amounts to several nanoseconds or to fractions of a nanosecond. A characteristic of a discharge of this type is that the time during which the electron avalanche grows to its critical size is commensurate with or shorter than the average lifetime of the excited gas molecules. In addition, the critical number of electrons and the corresponding number of excited molecules in the avalanche are themselves decreased with increasing applied electric field. This decreases greatly the yield of the photons from the avalanche and leaves its imprint on the entire discharge process.

First, the discharge loses its streamer character in the sense that the avalanche initiated by one or several electrons does not lead to the production of a streamer and to its transformation into a discharge channel. To complete the discharge in this case, a large number of electron avalanches must be produced by photoelectrons from the cathode. In this sense, a pulsed nanosecond discharge has many features in common with a Townsend discharge. Unlike the latter, however, the electron avalanche develops exponentially only during a very short time, after which, owing to the presence of the ion space-charge field, the rate of multiplication of the particles in the avalanche decreases. Then, as a result of the formation of new electrons ahead of the avalanche, an avalanche chain is produced, in which the growth of the number of electrons with time can be regarded as linear.

Second, a gas-gap current comparable with the maximum current determined by the discharge-circuit parameters is produced in such a discharge even before spark channels are produced in the gap. Such a space charge is observed in air, nitrogen, etc. up to pressures of several atmospheres, within a time of several dozen nanoseconds.

Third, after a large value of the current is reached in the gap, one observes in the gap the formation of not one but of a large number of spark channels. The reason for the formation of the channels has not yet been established, and the processes in them have not been investigated.

The picture changes appreciably if the number of electrons initiating the discharge is increased. In multielectron initiation, a space-charge current comparable with the maximum circuit current can be obtained without participation of secondary processes only through development of primary electron avalanches. Of particular interest is a discharge initiated by a beam of fast electrons. In this case, the space charge at a gas pressure up to several dozen atmospheres can be obtained even at a gap voltage much lower than the static breakdown voltage.

A discharge of this type can be used to excite gas lasers operating at high pressures. It is therefore

necessary to investigate in the future the conditions for optimal energy transfer from the storage device to the volume of the discharge.

At a gap field intensity exceeding 10^5 V/cm, a number of new phenomena begin to appear in a gas discharge. First, at large E/p the energy lost by the electron becomes smaller than the energy acquired by it from the field. This leads to a progressive acceleration of the electrons and to their "runaway" from the avalanche, and is manifest by x-ray emission from the anode. Second, discharge can influence effect characteristics of vacuum breakdown, such as electric explosion of microscopic sharp points on the cathode and the appearance of explosion emission of the electrons. This type of discharge, however, has been little investigated so far.

[1] L. B. Loeb, Basic Processes of Gaseous Electronics, U. of Cal., 1955, Chap. 5.

[2] J. M. Meek and J. D. Craggs, Electrical Breakdown of Gases, Oxford, 1953.

[3] H. Raether, Electron Avalanches and Breakdown in Gases, Butterworths, 1964.

[4] G. A. Vorob'ev and G. A. Mesyats, Tekhnika formirovaniya vysokovol'tnykh nanosekundnykh impul'sov (Technique of High-voltage Nanosecond Pulse Formation), M., Atomizdat, 1963, Chaps. III-IV.

[5] K. Vollrath and G. Thomer, translation in: Fizika bystroprotekayushchikh protsessov (Physics of Rapid Processes), Mir, 1971, p. 96.

[6] S. C. Brown, Elementary Processes in Gas-discharge Plasma (Russ. transl.), Atomizdat, 1961, Chap. 3.

[7] H. Schlumbohm, Zs. Phys. 182, 317 (1965).

[8] H. Schlumbohm, ibid. 184, 492 (1965).

[9] W. Sroka, Phys. Lett. 14, 301 (1965).

[10] A. Przybylski, Zs. Phys. 168, 504 (1962): G. W. Penney and R. E. Voshall, Trans. Am. Inst. Elec. Engrs. 1, 398 (1962); W. Bemert and H. Felt, Zs. angew. Phys. 8, 424 (1956); A. Przybylski, Zs. Phys. 151, 264 (1958).

[11] T. H. Teich, ibid. 199, 378 (1967).

[12] T. H. Teich, ibid., S. 395.

[13] W. Legler, ibid. 143, 173 (1955).

[14] K. Wagner, Zs. Naturforsch. 19a, 516 (1964); H. Akton, Ann. Phys. 18, 178 (1966).

[15] G. A. Mesyats, A. M. Iskol'skiĭ, V. V. Kremnev, L. G. Bychkova, and Yu. I. Bychkov, Zh. Prikl. Mat. Tekh. Fiz., No. 3, 77 (1968).

[16] V. V. Kremnev, T. A. Mesyats, and Yu. B. Yankelevich, Izv. vuzov (Fizika) No. 2, 81 (1970).

[17] K. J. Schmidt-Tiedeman, Zs. Naturforsch. 14a, 989 (1959).

[18] J. Maurel et al., C. R. Ac. Sci. A266, 1390 (1968).

[19] K. Richter, Zs. Phys. 180, 489 (1964).

[20] H. Tholl, Zs. Naturforsch. 18a, 587 (1963).

[21] R. Strigel, Elektrische Stossfestigkeit, B., Springer-Verlag, 1952.

[22] L. Malter, Phys. Rev. 49, 879 (1936); H. Paetow, Zs. Phys. 111, 770 (1939).

[23] Ékzoelektronnaya émissia, (Exoelectronic Emission) (translations) IL, 1962.

[24] M. I. Elinson and G. F. Vasil'ev, Avtoeléktronnaya émissiya (Field Emission), M., Fizmatgiz, 1958, Chap. 2.

[25] I. N. Slivkov et al., Élektricheskiĭ proboi i razryad v vakuume, (Electric Breakdown and Discharge in Vacuum), Atomizdat, 1966; Chaps. II and IV; W. Schottky, Zs. Phys. 14, 63 (1923).

[26] R. P. Little and W. T. Whitney, J. Appl. Phys. 34, 2430 (1963).

[27] G. A. Bogdanovskiĭ, Fiz. Tverd Tela 1, 1281 (1959). [Sov. Phys.-Solid State 1, 1171 (1960)].

[28] R. V. Latham and E. Braun, Proc. of the 3rd International Symposium of Discharges and Electrical Insulation in Vacuum, P., 1968, p. 123.

[29] K. Kerner, Zs. angew. Phys. 8, 1 (1956).

[30] A. J. Robertson et al. Brit. J. Appl. Phys. 14, 278 (1963).

[31] C. J. Bennete et al., Amer. Inst. Aeronaut, Astronaut. 3, 284 (1965).

[32] D. Alpert et al., J. Vacuum Sci. Technol. 1, 35 (1964).

[33] Yu. L. Stankevich, Zh. Tekh. Fiz. 40, 1476 (1970) [Sov. Phys.-Tech. Phys. 15, 1138 (1971)].

[34] Yu. L. Stankevich and M. S. Kalinin, Dokl. Akad. Nauk SSSR 177, 72 (1967) [Sov. Phys.-Doklady 12, 1042 (1968)].

[35] G. A. Mesyats and Yu. I. Bychkov, Zh. Tekh. Fiz. 37, 1712 (1967) [Sov. Phys. Tech.-Phys. 12, 1255 (1968)].

[36] G. A. Mesyats, Yu. I. Bychkov, and A. M. Iskol'dskiĭ, ibid. 38, 1281 (1968) [13, 1051 (1969)].

[37] R. C. Fletcher, Phys. Rev. 76, 1501 (1949).

[38] D. Goodal and R. Hancocs, Proc. of the 6th Intern. Conference on Phenomena in Ionized Gases, Paris, 1963, p. 337.

[39] L. G. Bychkova, Yu. I. Bychkov, and G. A. Mesyats, Izv. vuzov (Fizika), No. 2, 36 (1969).

[40] G. A. Mesyats and Yu. I. Bichkov, 9th Intern. Conference on Phenomena in Ionized Gases, Bucharest, 1969, p. 262.

[41] Yu. I. Bychkov and L. G. Bychkova, Élektronnaya tekhnika, ser. 3, No. 2, 39 (1967).

[42] Yu. E. Nesterikhin et al., Zh. Tekh. Fiz. 34, 40 (1964) [Sov. Phys.-Tech. Phys. 9, 29 (1964)].

[43] V. V. Kremnev and G. A. Mesyats, Zh. Prikl. Mat. Tekh. Fiz. No. 1, 40 (1971).

[44] V. V. Vorob'ev and A. M. Iskol'dskiĭ, Zh. Tekh. Fiz., 36, 2095 (1966) [Sov. Phys.-Tech. Phys. 11, 1560 (1967)].

[45] L. G. Bychkova, Yu. I. Bychkov, G. A. Mesyats, and Ya. Ya. Yurike, Izv. vuzov (Fizika), No. 11, 24 (1969).

[46] Yu. I. Bychkov et al., Zh. Tekh. Fiz. 42, No. 7 (1972) [Sov. Phys.-Tech. Phys. 17, No. 7 (1973)].

[47] G. A. Mesyats, Ya. I. Bychkov, and Yu. D. Korolev, 10th Intern. Conference on Phenomena in Ionized Gases, Oxford, 1971, p. 168.

[48] Yu. I. Bychkov et al., Trudy IV Vsecoyuznoĭ konferentsii po fizike i generatoram nizkotemperaturnoĭ plazmy (Proc. 4-th All-union Conf. on Physics and Low-temp. Plasma Generators), Alma-Ata, Kazakh. Polytech. Inst. 1970, p. 460.

[49] I. P. Afonin et al., PTE, No. 2, 138 (1971).

[50] G. A. Mesyats and V. V. Kremnev, et al., Zh. Tech. Fiz. 39, 75 (1969) [Sov. Phys.-Tech. Phys. 14, 49 (1969)].

[51]Yu. E. Nesterikhin and P. I. Soloukhin, Metody skorostnykh izmerenii v gazodinamike i fizike plazmi (Methods of High-speed Measurements in Gasdynamics and Plasma Physics), Nauka, 1967, Chaps. III and V.
[52]F. R. Dickey, J. Appl. Phys. 23, 1336 (1952).
[53]P. Felsenthal and J. M. Proud, Phys. Rev. 139, 1796 (1965).
[54]R. C. Fletcher, Rev. Sci. Instr. 20, 12 (1949).
[55]Yu. P. Usov, Candidate's dissertation, Tomsk Polytech, Inst. 1963.
[56]B. M. Koval'chuk, V. V. Kremnev, and G. A. Mesyats, Dokl. Akad. Nauk. SSSR 191, 76 (1970) [Sov. Phys.-Doklady 15, 267 (1970)].
[57]T. F. Godlove, J. Appl. Phys. 32, 1589 (1961).
[58]S. Stolen, cm.[40], p. 259.
[59]B. M. Koval'chuk, V. V. Kremnev, and G. A. Mesyats, Yu. F. Potalitsyn, Zh. Prikl. Mat. Tekh. Fiz., No. 6, 21 (1971).
[60]N. G. Basov et al., Kvantovaya elektronika, No. 3, 121 (1971) [Sov. J. Quant Electron. 0, 000 (197)]; A. K. Laflamme, Rev. Sci. Instr. 41, 1578 (1970).
[61]G. A. Mesyats and D. I. Proskurovskiĭ, ZhETF Pis. Red. 13, 7 (1971) [JETP Lett. 13, 4 (1971)].
[62]G. K. Kartsev and G. A. Mesyats, et al., Dokl. Akad. Nauk SSSR, 192, 309 (1970) [Sov. Phys.-Doklady 15, 475 (1970)].
[63]A. V. Gurevich, Zh. Eksp. Teor. Fiz. 39, 1296 (1960) [Sov. Phys.-JETP 12, 904 (1961)].
[64]S. V. Starodubtsev and L. M. Romanov, Prokhozhdenie zaryazhennykh chastits cherez veshchestvo (Penetration of Charged Particles through Matter), Tashkent, AN Uzb. SSR, 1951.
[65]R. C. Noggle, et al., J. Appl. Phys. 39, 4746 (1968).
[66]V. V. Kremnev and Yu. A. Kyrbatov, Zh. Tekh. Fiz. 42, 795 (1972) [Sov. Phys.-Tech. Phys. 17, 626 (1972)].

Translated by J. G. Adashko